Very low frequency modulation in QRS slopes and its relation with respiration and heart rate variability during hemodialysis

David Hernando, Alejandro Alcaine, Pablo Laguna, Esther Pueyo and Raquel Bailón

Abstract— In this work, we study the very low frequency (VLF) modulation (range 0.01-0.03 Hz) in QRS slopes, heart rate variability (HRV) and ECG-derived respiration in hemodialysis patients. First, the relation between QRS slopes and HRV in the VLF band is measured using ordinary coherence. Then, partial coherence is used to measure the former relationship once the effect related to respiration is removed. Ordinary coherence values above a statistical threshold revealed linear relationship between VLF modulation in QRS slopes and HRV in about 10% of analyzed segments, with mean $\pm$ SD values of 0.79 $\pm$ 0.07 for upward slope and 0.77 $\pm$ 0.06 for downward slope. For these segments, partial coherence values drop below the threshold for 64% of the cases for upward slope and 76% for downward slope, suggesting that the origin of the VLF modulation in QRS slopes is mainly driven by respiration or linearly related to it. In the rest of the cases, partial coherence values dropped with respect to ordinary coherence from 0.89 to 0.77 for upward slope and from 0.86 to 0.75 for downward slope, suggesting that other ANS effects non-linearly related to respiration also contribute to the VLF modulation in QRS slopes.

I. INTRODUCTION

Spectral analysis of heart rate variability (HRV) is a non-invasive tool which assesses changes of the autonomic nervous system (ANS) and the sympatho-vagal balance. Three bands are established in the power spectrum of HRV at rest [1]: very low frequency (VLF: < 0.04 Hz), low frequency (LF: 0.04 to 0.15 Hz) and high frequency (HF: 0.15 to 0.4 Hz). The behaviour in the HF and LF bands are well known: the HF component is considered to be a marker of the parasympathetic activity, being synchronous with respiration, and the LF component is a marker of the sympathetic modulation, at least when measured in normalized units. However, the mechanisms which modulate the VLF component are more controversial. It has been linked with humoral and temperature regulation [2], with slow vasomotor activity or with parasympathetic outflow [3].

QRS slopes are used to analyze depolarization changes induced by ischemia on the electrocardiogram (ECG), as they are very sensitive to the changes in the QRS morphology [4].

In patients with stable angina pectoris, a VLF modulation was found out in QRS slopes series, both upwards and downwards [5], synchronous with the VLF component of HRV [6]. The origin of this modulation is unclear. Moreover, in patients with renal failure a VLF modulation in HRV as well as in ECG-derived respiration has been observed during hemodialysis [7].

In this work we study the VLF modulation in QRS slopes and HRV in hemodialysis patients. Our hypothesis is that the source of that modulation is respiration, either directly or through ANS which controls respiration, and that other non linearly related autonomic regulation effects are secondary.

First, the relation between QRS slopes and HRV in the VLF band is measured using ordinary coherence. Then, partial coherence is used to measure the relation between QRS slopes and HRV once the effect of respiration is removed. Finally, partial coherence is compared to ordinary coherence to find out if respiration influence is the main origin of the VLF modulation in QRS slopes series.

II. METHODS AND MATERIALS

A. Study population

The database used in this work consist of 16 patients (12 men) with renal failure who underwent regular hemodialysis three times a week. The average age is 62.5 $\pm$ 11.8 years. A total of 30 sessions were acquired during the entire clinical treatment at Park Dialys, Lund, Sweden, and Helsingborg Hospital, Helsingborg Sweden, lasting from 3 to 5 hours.

In these sessions the standard 12 lead ECG was acquired and digitalized at a sampling rate of 1000 Hz and amplitude resolution of 0.06 μV (Siemens-Elema AB, Sweden). The subsequent analysis was performed in 5-minute segments where stationarity of the ECG signal was assumed.

B. QRS slopes

First, the QRS complex were detected from the ECG signal using ARISTOTLE [8] and then the ECG was pre-processed to attenuate the baseline via cubic spline interpolation. The vectorcardiogram (VCG) was computed using the inverse Dower matrix to obtain three ortogonal leads: $x(n)$, $y(n)$ and $z(n)$, which represents the movement of the heart's electric vector in the space.

Yet another lead called *loop derived lead* is considered, aiming to better catch the respiration effect on the ECG, since this leadhas the maximum level of signal-to-noise ratio (SNR). First, the dominant direction $\boldsymbol{u}$ of each QRS complex is determined as:

$$\boldsymbol{u} = [u_{\mathrm{x}}, u_{\mathrm{Y}}, u_{\mathrm{z}}]^T = [x(n_0), y(n_0), z(n_0)]^T \qquad (1)$$

with

$$n_0 = \operatorname*{argmax}_{n} \left[x^2(n) + y^2(n) + z^2(n) \right] \qquad (2)$$

where n spans from 20 ms before to 130 ms after each QRS complex onset. The loop derived lead $l(n)$ is calculated by projecting the points of the QRS loop onto this $\boldsymbol{u}$ axis [5].

$$l(n) = \frac{[x(n), y(n), z(n)]^T \, \boldsymbol{u}}{||\boldsymbol{u}||} \qquad (3)$$

These four leads are delineated using a wavelet-based technique [9] to determine both the onset and offset of the QRS complex, and Q, R and S peaks position. QRS slopes are calculated using the algorithm presented in [4], obtaining the slope indices: I_{US} for the upward slope and I_{DS} for the downward slope of the R wave for each beat. All the beats in a segment resampled at 4 Hz leads to the $I_{\mathrm{US}}(n)$ and $I_{\mathrm{DS}}(n)$ signals. $I_{\mathrm{XS}}(n)$ will be used from now on to denote any of the two slope signals.

C. Heart rate variability

The HRV signal is derived from the QRS detection marks, following a method based on the Integral Pulse Frequency Modulation (IPFM) model [10], and resampled at 4 Hz obtaining $d_{\mathrm{HR}}(n)$. The ectopic beats and misdetections are located and corrected using [11].

D. ECG-derived respiration

Since no reference respiratory signal is available, and EDR signal is used instead. In this work, the EDR signals are the heart electrical axis rotation angle series, obtained by the spatio-temporal alignment of successive QRS-VCG loops [12]. The three rotation angles are resampled at 4Hz and denoted: $\phi_{\mathrm{x}}(n)$, $\phi_{\mathrm{Y}}(n)$ and $\phi_{\mathrm{z}}(n)$.

E. Ordinary spectral coherence and partial spectral coherence

Ordinary spectral coherence is used to measure the degree of linear relationship between two signals i and j:

$$\gamma_{ij}(f) = \frac{S_{ij}(f)}{\sqrt{S_i(f) S_j(f)}} \qquad (4)$$

being $S_i(f)$ the power spectral density function of the signal i, and $S_{ij}(f)$ the cross-spectrum between signals i and j.

If there is a third signal k linearly related to signals i and j, partial coherence can be used to measure the degree of linear relationship between signals i and j, after removing the effect of k [13]. It is defined as:

$$\gamma_{ij|k}(f) = \frac{|S_{ij|k}(f)|}{\sqrt{S_{i|k}(f) S_{j|k}(f)}} \qquad (5)$$

with

$$S_{ij|k}(f) = S_{ij}(f) - \frac{S_{ik}(f) S_{kj}(f)}{S_k(f)} \qquad (6)$$

and

$$S_{i|k}(f) = S_i(f) - \frac{S_{ik}(f) S_{ki}(f)}{S_k(f)} \qquad (7)$$

The power spectral densities and the cross-spectra are estimated using the Minimum Variance Distortionless Response (MVDR) [14] to achieve higher spectral resolution than classical periodogram, which is needed especially in the study of the VLF modulation.

F. Statistical threshold

For the study of ordinary and partial coherences, a threshold must be determined to decide in which segments QRS slopes and HRV are linearly related in the VLF band. A fixed threshold can be misleading, since two uncorrelated signals present random coherence which is not equal to zero. Moreover, estimators used to calculate auto and cross-spectra also affect coherence values [15].

In this work, the statistical threshold ρ has been estimated as follows: ordinary coherence between two segments of white noise has been computed in the VLF band, using the same methods than the rest of the work. After 1000 repetitions, the maximum of the coherence in each iteration has been annotated and sorted. The percentile η % is chosen to obtain ρ, with an error of (100-η) %.

G. Segment selection

First, segments in which ordinary coherence between $I_{\mathrm{XS}}(n)$ and $d_{\mathrm{HR}}(n)$ is above the threshold are selected.

The next step is to include the EDR signal. Not every selected segment present the modulation in the EDR signal: ordinary coherence between EDR and $d_{\mathrm{HR}}(n)$, and between EDR and $I_{\mathrm{XS}}(n)$ is computed, if both coherece values are above the threshold, the frequencies associated to them coincide with the VLF modulation in $d_{\mathrm{HR}}(n)$ and $I_{\mathrm{XS}}(n)$, and the spectrum of the EDR signal is "peaky" enough, that segment is selected for the study. The spectrum is considered "peaky" if two conditions are fullfilled. First, that at least 50% of the total power in the VLF band is contained in an interval centered around the largest peak f_o: $[f_o\text{-}0.01\mathrm{Hz}, f_o\text{+}0.01\mathrm{Hz}]$. And second, that power spectral density values at the interval extremes do not exceed 75% of the value at f_o.

III. RESULTS

An example of the VLF modulation can be seen in Figures 1 and 2, where the HRV, QRS slopes and EDR signals are represented, in time (they have been low-pass filtered using a cut-off frequency of 0.15 Hz for representation) and frequency domain (power spectral density).

The statistical threshold corresponding to percentil 99% is $\rho = 0.7$. Segments in which ordinary coherence between $I_{\mathrm{XS}}(n)$ and $d_{\mathrm{HR}}(n)$ is above the threshold are selected.
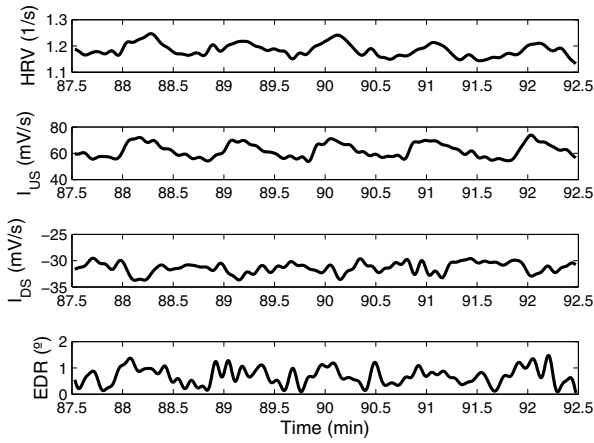
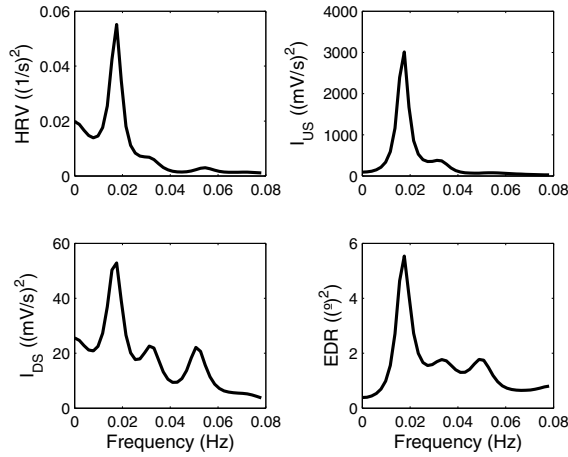Fig. 1.   VLF modulation in HRV, QRS slopes and EDR (time domain)

Fig. 2.   VLF modulation in HRV, QRS slopes and EDR (frequency domain)

TABLE I

VLF MODULATION IN HRV AND QRS SLOPES.

		$d_{\mathrm{HR}}(n)$–$I_{\mathrm{US}}(n)$	$d_{\mathrm{HR}}(n)$–$I_{\mathrm{DS}}(n)$
# Patients (# Segments)	$x(n)$	16 (184)	16 (145)
	$y(n)$	16 (162)	16 (147)
	$z(n)$	16 (134)	16 (149)
	$l(n)$	16 (186)	16 (181)
$\gamma_{ij}(f_o)$	$x(n)$	0.79 ± 0.06	0.78 ± 0.06
	$y(n)$	0.79 ± 0.06	0.78 ± 0.06
	$z(n)$	0.77 ± 0.05	0.77 ± 0.05
	$l(n)$	0.79 ± 0.07	0.77 ± 0.06

TABLE II

VLF MODULATION IN HRV, QRS SLOPES AND EDR.

		$d_{\mathrm{HR}}(n)$–$I_{\mathrm{US}}(n)$	$d_{\mathrm{HR}}(n)$–$I_{\mathrm{DS}}(n)$
# Patients (# Segments)	$x(n)$	7 (50)	8 (46)
	$y(n)$	6 (45)	7 (43)
	$z(n)$	7 (21)	8 (28)
	$l(n)$	8 (53)	9 (46)
$\gamma_{ij}(f_o)$	$x(n)$	0.83 ± 0.06	0.81 ± 0.06
	$y(n)$	0.83 ± 0.06	0.80 ± 0.06
	$z(n)$	0.79 ± 0.06	0.80 ± 0.05
	$l(n)$	0.84 ± 0.07	0.81 ± 0.07

$d_{\mathrm{HR}}(n)$ and $I_{\mathrm{XS}}(n)$. Figure 3 shows an example using the signals from Figures 1 and 2: the peak of the modulation in $d_{\mathrm{HR}}(n)$-$I_{\mathrm{US}}(n)$ drops in partial coherence compared to ordinary coherence, from 0.92 to 0.64, becoming below the threshold.
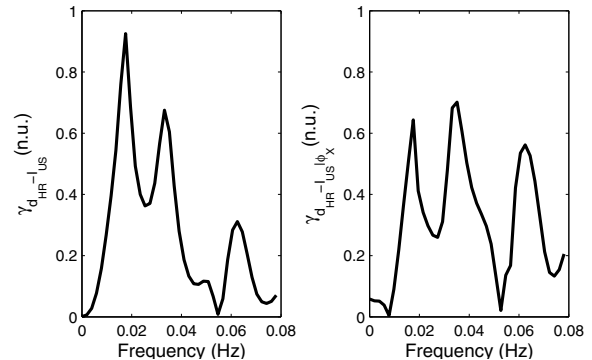

Fig. 3.   Example of decrease of VLF modulation peak in partial coherence.

The lead $l(n)$ presents higher percentage of segments with modulation. For $I_{\mathrm{US}}(n)$, 34 segments present partial coherence values which are below the threshold, indicating that the linear relation between $I_{\mathrm{XS}}(n)$ and $d_{\mathrm{HR}}(n)$ was explained by their linear relation with respiration as measured by $\phi_{\mathrm{x}}(n)$. The other segments present partial coherence values of 0.77 ± 0.06 versus ordinary coherence value of 0.89 ± 0.04. In these cases, there is still linear relation between $I_{\mathrm{XS}}(n)$ and $d_{\mathrm{HR}}(n)$ which is not due to the influence of $\phi_{\mathrm{x}}(n)$ and may be related to other ANS regulatory mechanisms.

For $I_{\mathrm{DS}}(n)$, 35 segments present partial coherence values which are below the threshold and the rest present partial coherence values of 0.75 ± 0.04 versus ordinary coherence value of 0.86 ± 0.05. These results can be seen in Table III.

It can be appreciated a notable decrease in partial coherence while comparing to ordinary coherence. A Kolmogorov-

To obtain $I_{\mathrm{XS}}(n)$, the four leads were considered, $x(n)$, $y(n)$, $z(n)$ and $l(n)$. As it can be seen in Table I, all patients present at least one segment with coherence values between $d_{\mathrm{HR}}(n)$ and $I_{\mathrm{XS}}(n)$ above ρ, but only in short periods of time. Beetween 134 and 186 segments are included, which represent the 8.37% and 10.41% of the total number of segments, respectively. The range of the mean value of the coherence in the VLF band, denoted as $\gamma_{ij}(f_o)$, is 0.77-0.79.

To remove the respiration influence, the EDR signal is included to the study. $\phi_{\mathrm{x}}(n)$ and $\phi_{\mathrm{z}}(n)$ lead to similar results, while $\phi_{\mathrm{Y}}(n)$ leads to worse results. For that reason, only the results with $\phi_{\mathrm{x}}(n)$ will be shown here.

Including $\phi_{\mathrm{x}}(n)$, several segments are rejected due to the absence of the VLF modulation in the EDR signal, as described in II-G. As the Table II shows, only 6-9 patients present the VLF modulation in the three signals during 21-53 segments. The mean value of the coherence in this reduced set is larger than before: 0.79-0.84.

Within these segments, partial coherence is computed to remove the influence of $\phi_{\mathrm{x}}(n)$ in the linear relation between

TABLE III
SEGMENTS WHERE $\gamma_{ij|k}(f_o) < \gamma_{ij}(f_o)$ (VCG).

		$d_{HR}(n)-I_{US}(n)$	$d_{HR}(n)-I_{DS}(n)$
# Segments $\gamma_{ij|k}(f_o) < \rho$	$x(n)$	32	34
	$y(n)$	35	40
	$z(n)$	14	23
	$l(n)$	**34**	**35**
# Segments $\gamma_{ij|k}(f_o) > \rho$	$x(n)$	19	12
	$y(n)$	10	3
	$z(n)$	14	7
	$l(n)$	**19**	**11**
$\gamma_{ij|k}(f_o)$ vs $\gamma_{ij}(f_o)$	$x(n)$	0.79 vs 0.88	0.78 vs 0.87
	$y(n)$	0.77 vs 0.88	0.76 vs 0.9
	$z(n)$	0.77 vs 0.86	0.77 vs 0.84
	$l(n)$	**0.77 vs 0.89**	**0.75 vs 0.86**

Smirnov test is applied to these coherence values to find out whether the data follows a normal distribution or not. The result of this test is negative, so a KruskalWallis analysis is used to test equality of population medians among the ordinary and partial coherence values. For both $I_{US}(n)$ and $I_{DS}(n)$ the p-value is below 0.05, so the two groups are considered significantly distinct.

Similar results can be achieved using the three leads of VCG, which are also shown in Table III.

IV. DISCUSSION

The VLF modulation only appears in short periods of time in this database and it is very irregular, ranging from 5 minutes to one hour and a half, depending on the patient.

These very low frequency components in HRV have been associated to the modulation observed in periodic breathing [16]. This phenomenon also affects QRS morphology, which can be studied by analyzing QRS slopes, and it has been reported a relation on the VLF modulation between both [6]. In this work it has been proved that respiration has indeed influence in such modulation.

Regarding the loop derived lead, 64.15% of the segments present a drop in the partial coherence below the threshold comparing to ordinary coherence in the case of the upward slope, and 76% in the case of the downward slope, which suggests that respiration is strongly related to the modulation. The segments that have lower partial coherence values than ordinary coherence ones but still higher than the threshold, present a drop of more than 10%. This means that respiration is not the only source of this modulation, being possibly other effects of the autonomic nervous system responsible as well.

The main limitation in this work is the ausence of the direct respiratory signal. EDR signals have been reported to estimate acurately respiratory frequency [12], but their performance has not been evaluated in the VLF band. A reference respiration signal would be needed to confirm these results.

Note that these results are obtained from a database composed of elderly renal failure patients, whose age, pathology and medication affect ANS regulation over the heart, and may also affect the relationship between QRS slopes, respiration and HRV.

V. CONCLUSION

In this work, ordinary coherence in the VLF band between HRV and QRS slopes has been computed. Then, partial coherence has been performed to analyze the respiration influence, using a ECG-derived respiration signal. It has been shown a significative drop in partial coherence compared to ordinary coherence and this points that the mayority of the relation between HRV and QRS slopes can be explained by a coherent linear effect of respiration, which agrees the initial hypotesis. The remaining needs to be analyzed as an alternative effect, or due to the use of the EDR signal rather than true respiration.

REFERENCES

[1] T. T. F. of ESC and NASPE, "Heart rate variability. standards of measurement, physiological interpretation, and clinical use," *Eur. Heart J.*, vol. 17, pp. 354–381, 1996.

[2] R. I. Kitney, "The use of entrainment in the analysis of the human thermoregulatory system," *J Physiol*, vol. 229, no. 1, pp. 40–41, 1973.

[3] K. K. Tripathi, "Very low frequency oscillations in the power spectra of heart rate variability during dry supine immersion and exposure to non-hypoxic hypobaria," *Physiol Meas.*, vol. 32, no. 6, pp. 717–729, 2011.

[4] E. Pueyo, L. Sörnmo, and P. Laguna, "QRS slopes for detection and characterization of myocardial ischemia," *IEEE Transactions on Biomedical Engineering*, vol. 55, no. 2, pp. 468–477, 2008.

[5] D. Romero, M. Ringborn, P. Laguna, and E. Pueyo, "Depolarization changes during acute myocardial ischemia by evaluation of QRS slopes: standard lead and vectorial approach," *IEEE Transactions on Biomedical Engineering*, vol. 58, no. 1, pp. 110–120, 2011.

[6] A. Alcaine, R. Bailón, D. Romero, E. Pueyo, and P. Laguna, "Very-low-frequency modulation of qrs slopes in patients with angina pectoris," in *Computers in Cardiology 2011*, 2011, pp. 757–760.

[7] D. Hernando, R. Bailón, P. Laguna, and L. Sörnmo, "Heart rate variability analysis during hemodialysis and its relation with hypotension," in *Computers in Cardiology 2011*, 2011, pp. 189–192.

[8] G. B. Moody and R. Mark, "Development and evaluation of a 2-lead ecg analysis program," in *Computers in Cardiology 1982*, 1982, pp. 39–44.

[9] J. P. Martínez, R. Almeida, S. Olmos, A. P. Rocha, and P. Laguna, "A wavelet-based ecg delineator: Evaluation on standard databases," *IEEE Transactions on Biomedical Engineering*, vol. 51, no. 4, pp. 570–581, 2004.

[10] J. Mateo and P. Laguna, "Improved heart rate variability signal analysis from the beat occurrence times according to the IPFM model," *IEEE Transactions on Biomedical Engineering*, vol. 47, no. 8, pp. 985–996, 2000.

[11] J. Mateo and P. Laguna, "Analysis of heart rate variability in the presence of ectopic beats using the heart timing signal," *IEEE Transactions on Biomedical Engineering*, vol. 50, no. 3, pp. 334–343, 2003.

[12] R. Bailón, L. Sörnmo, and P. Laguna, "A robust method for ECG-based estimation of the respiratory frequency during stress testing," *IEEE Transactions on Biomedical Engineering*, vol. 53, no. 7, pp. 1273–1285, 2006.

[13] J. Bendat and A. Piersol, *Random Data: Analysis and Measurement Procedures*, J. W. . Sons, Ed. Wiley Series in Probability and Statistics, 2010.

[14] J. Benesty, J. Chen, and Y. Huang, "Estimation of the coherence function with the MVDR approach," *Proc. IEEE Int. Conference on Acoustics, Speech and Signal Processing (ICASSP)*, vol. 3, 2006.

[15] L. Faes, G. D. Pinna, A. Porta, R. Maestri, and G. Nollo, "Surrogate data analysis for assessing the significance of the coherence function," *IEEE Transactions on Biomedical Engineering*, vol. 51, pp. 1156–1166, 2004.

[16] D. P. Francis, K. Willson, L. C. Davies, A. J. Coats, and M. Piepoli, "Quantitative general theory for periodic breathing in chronic heart failure and its clinical implications," *Circulation*, vol. 102, no. 18, pp. 2214–2221, 2000.